Supporting Information

Enabling Superprotonic Phase Transitions in Solid Acids Via Supramolecular Complex Formation: The Case of Crown Ethers and Alkali Hydrogensulfates

Samet Ocak,[a] Simone d'Agostino,[a]* Grega Venturini,[a] Francesca Soavi,[a]* Simone Bordignon,[b] Michele R. Chierotti,[b]* and Dario Braga[a]

[a] Department of Chemistry "Giacomo Ciamician", Alma Mater Studiorum Università di Bologna, Via F. Selmi, 2, 40126 Bologna, Italy.

[b] Dipartimento di Chimica and NIS Centre, University of Torino, Via P. Giuria, 7, 10125 Torino, Italy

Table of contents

Crystal data and refinement details	S-2
Crystal structure description of **2**·2H2O	S-3
Comparison between Ortep drawing for 1 at RT and at 90 °C	S-3
Coordination and hydrogen bond interactions	S-4
Powder XRD pattern - Phase identification	S-4
Thermal Analyses	S-5
Variable-temperature powder XRD	S-7
EIS details and Arrhenius plots	S-8
Solid-state NMR	S-10

Crystal data and refinement details.

Table S-1. Crystal data and refinement details for: **1** at RT and 90 °C, **2**·2H_2O**,** and **2** at RT and –170 °C.

	1 at RT	**1 at 90 °C**	**2·2H_2O**	**2 at RT**	**2 at –170 °C**
Formula	$C_{12}H_{25}KO_{10}S$	$C_{12}H_{25}KO_{10}S$	$C_{12}H_{29}RbO_{12}S$	$C_{12}H_{25}RbO_{10}S$	$C_{12}H_{25}RbO_{10}S$
FW (g/mol)	400.48	400.48	482.88	445.84	446.85
Crystal System	Monoclinic	Monoclinic	Monoclinic	Monoclinic	Triclinic
Space Group	$P2_1/n$	$P2_1/n$	Cc	$P2_1/n$	$P\bar{1}$
a/Å	10.2575(5)	10.268(2)	14.3347(9)	11.8135(4)	8.4019(9)
b/Å	8.4856(4)	8.5730(17)	17.7766(12)	8.5169(3)	11.7059(12)
c/Å	21.6092(8)	21.818(4)	8.3577(5)	19.5206(7)	19.105(2)
α/°	90	90	90	90	77.593(9)
β/°	99.229(4)	99.16(3)	100.929(7)	104.836(4)	89.118(9)
γ/°	90	90	90	90	86.333(9)
Volume/Å^3	1856.54(14)	1896.1(7)	2091.1(2)	1898.58(12)	1831.4(3)
Z	4	4	4	4	4
ρcalc g/cm^3	1.433	1.403	1.534	1.560	1.621
μ/mm^{-1}	0.44	0.412	2.521	2.762	2.86
measd rflns	8595	5265	4429	8418	12542
indep rflns	4246	2583	3275	4381	4095
R_1	0.0729	0.0473	0.0446	0.0403	0.0815
wR_2	0.2031	0.1526	0.0879	0.0662	0.1540

Crystal structure description of $2{\cdot}2H_2O$

Single-crystal analysis shows that in **2**·$2H_2O$ the HSO_4^- anions feature disorder over two positions, the overall structure is isostructural to the already reported potassium supramolecular complex[1] and it is characterized by the presence of chains of HSO_4^- anions linked by hydrogen bonds via the water molecules, while the rubidium cation is coordinated by the crown ether oxygen atoms (see Figure S-1).

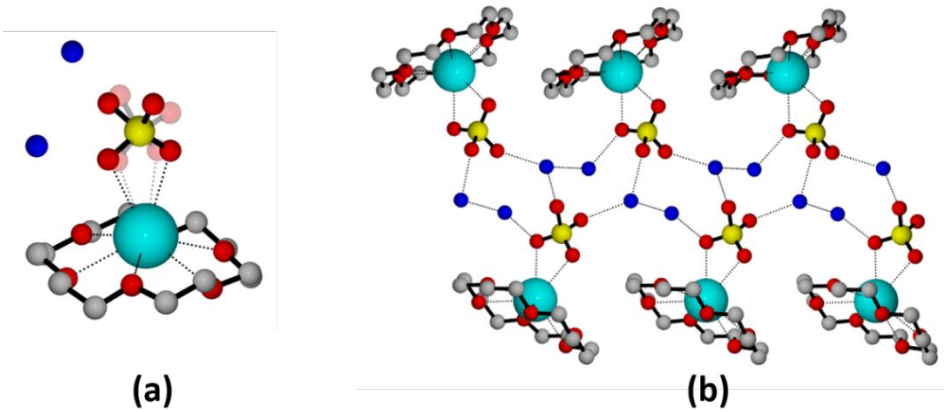

Figure S-1. (a) The asymmetric unit of **2**·$2H_2O$ showing the disorder affecting the HSO_4^- anion (second component in orange), and (b) crown ethers and ions organization detected within crystalline **2**·$2H_2O$ (disorder not shown). O_{water} in blue and H atoms omitted for clarity.

Comparison between Ortep drawing for 1 at RT and at 90 °C

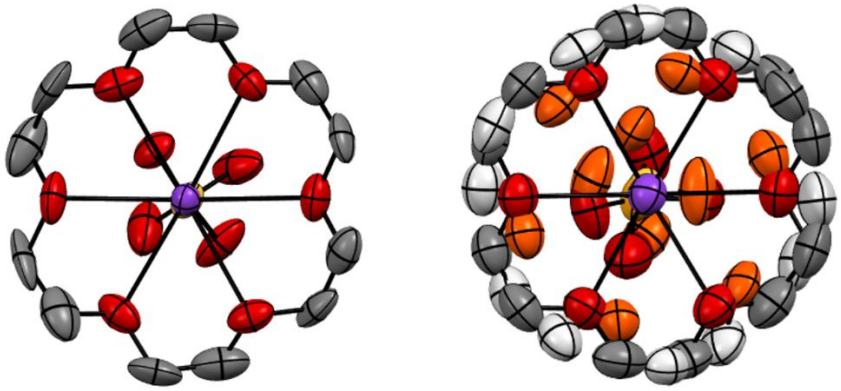

Figure S-2. Top views of the ortep drawings (50% probability) of **1** at RT (left) and at 90 °C (right). The second positions of C and O atoms are depicted in light grey and orange. H atoms omitted for clarity.

Coordination and hydrogen bond interactions

Table S-2. Metal coordination distances and hydrogen bonding interactions detected within crystalline **1** at 90 °C, **2**·2H_2O**, 2,** and **2** at –170 °C**.**

	1 at 90 °C	**2·2H_2O**	**2**	**2 at –170 °C**
K^+ ··· O_{crown}	2.726(11) – 3.008(5)	-	-	-
Rb^+ ··· O_{crown}	-	2.864(6) – 3.049(6)	2.916(2) – 3.112(2)	2.875(6) – 3.093(7)
K^+ ··· $O_{sulfate}$	2.778(18) – 3.002(19)	-	-	-
Rb^+··· $O_{sulfate}$	-	2.944(12) – 2.952(16)	2.956(11) – 3.14(2)	2.88(1) – 3.028(7)
H-bond ($O_{sulfate}$··· $O_{sulfate}$)	2.57(2) – 2.67(2)	-	2.38(3) – 2.67(2)	2.541(6) – 2.985(13)
H-bond ($O_{sulfate}$··· $O_{sulfate}$)	-	2.50(4) – 2.85(2)	-	-

Powder XRD pattern - Phase identification

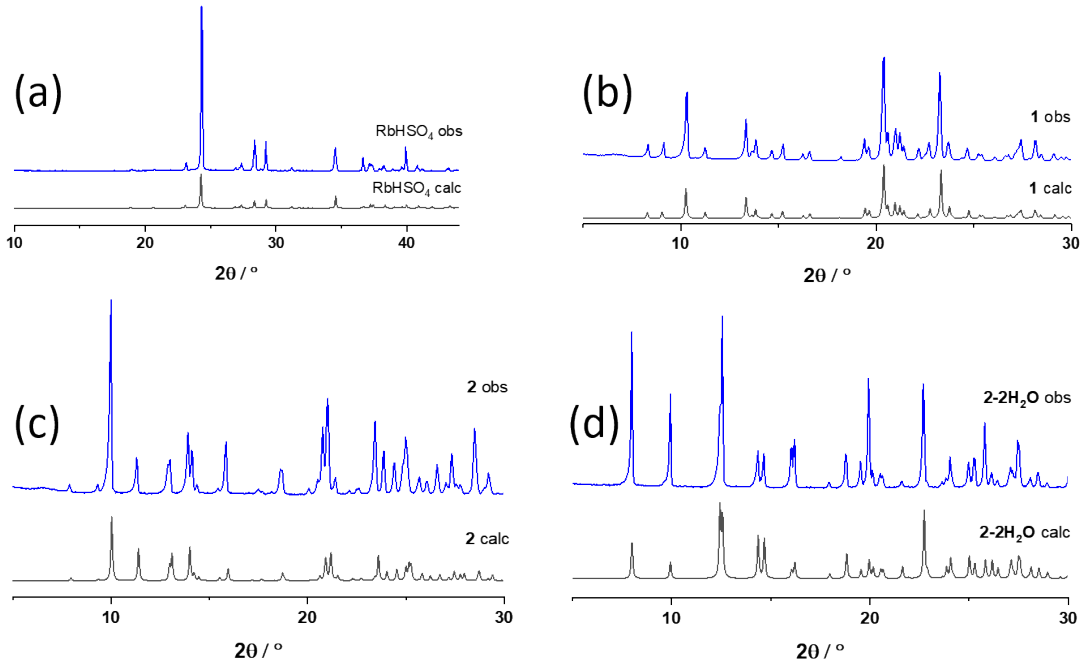

Figure S-3. Comparison between experimental (blue) and calculated patterns (black): (a) $RbHSO_4$, (ICSD ref code: 55447),[2] and (b) **1**, (c) **2**·2H_2O and (d) **2**. $RbHSO_4$

Thermal Analyses

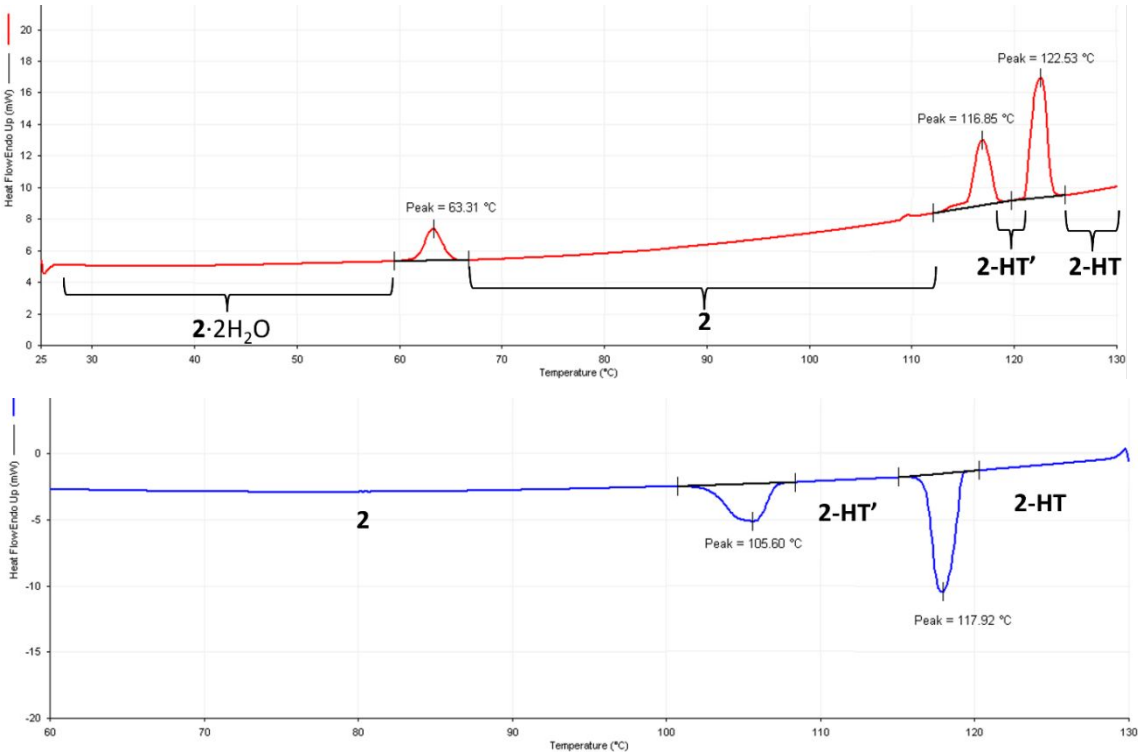

Figure S-4. DSC traces showing the phase changes **2**·2H_2O → **2** → **2**-HT'→ **2**-HT (red and blue lines represent the heating and cooling cycles).

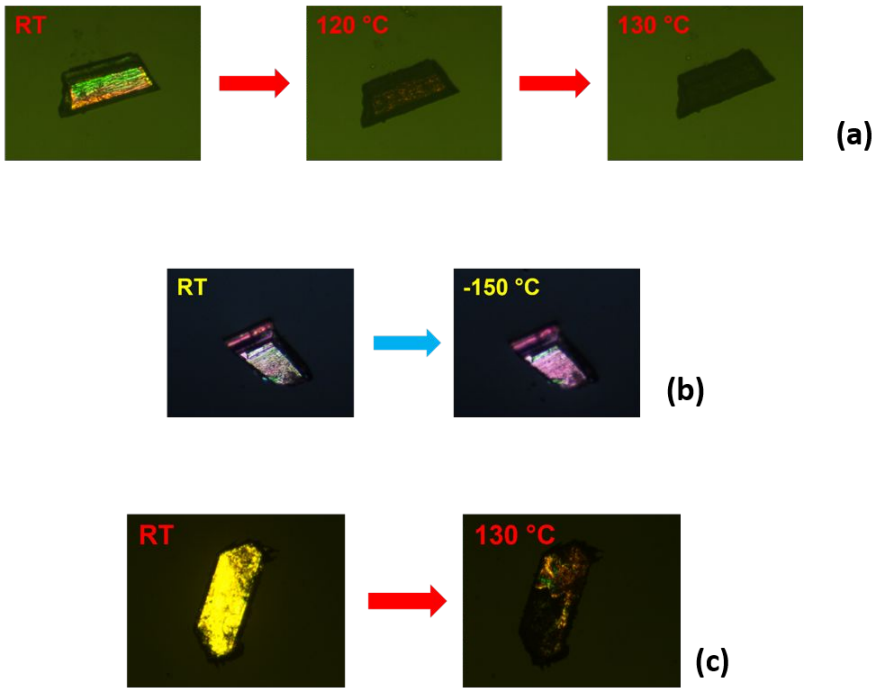

Figure S-5. Crossed Polarized Hot Stage Microscopy pictures of (a) **2** → **2**-HT'→ **2**-HT (b) **2** → **2**-LT (c) **1** → **1**-HT.

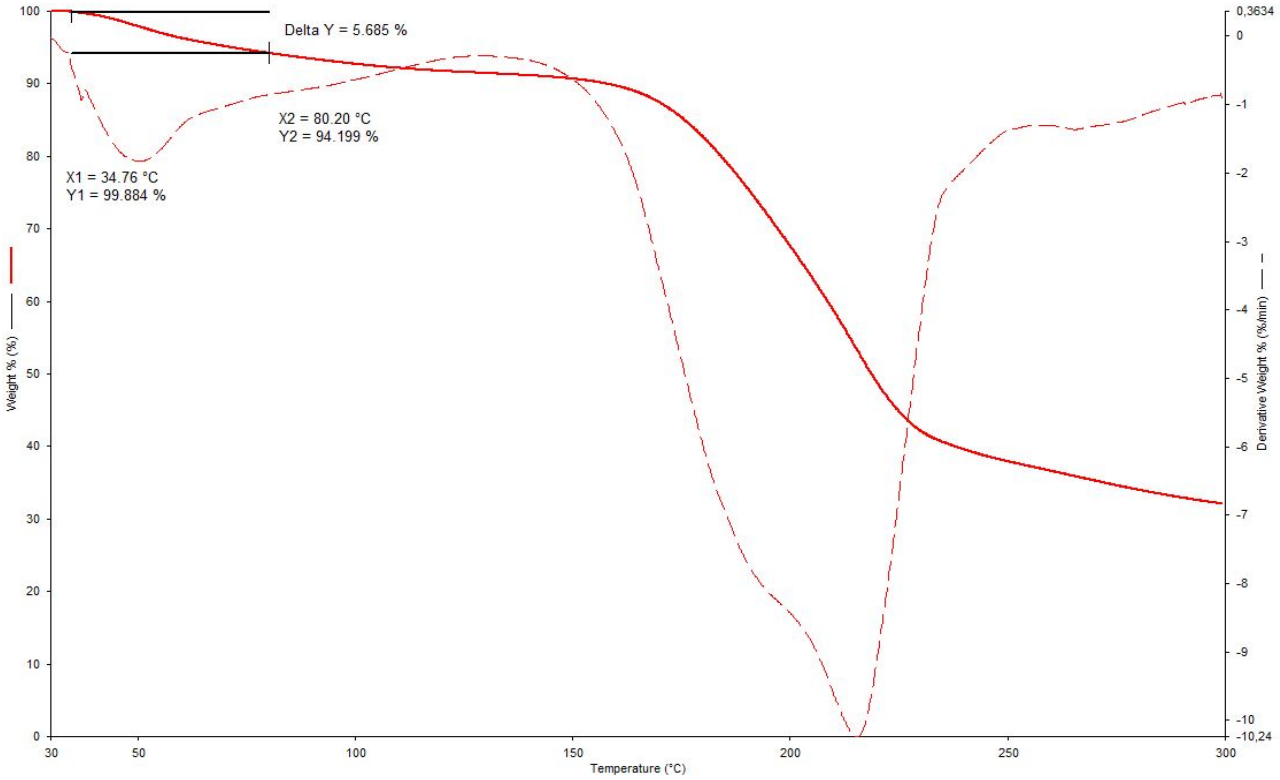

Figure S-6. TGA trace of **1**·2H_2O.

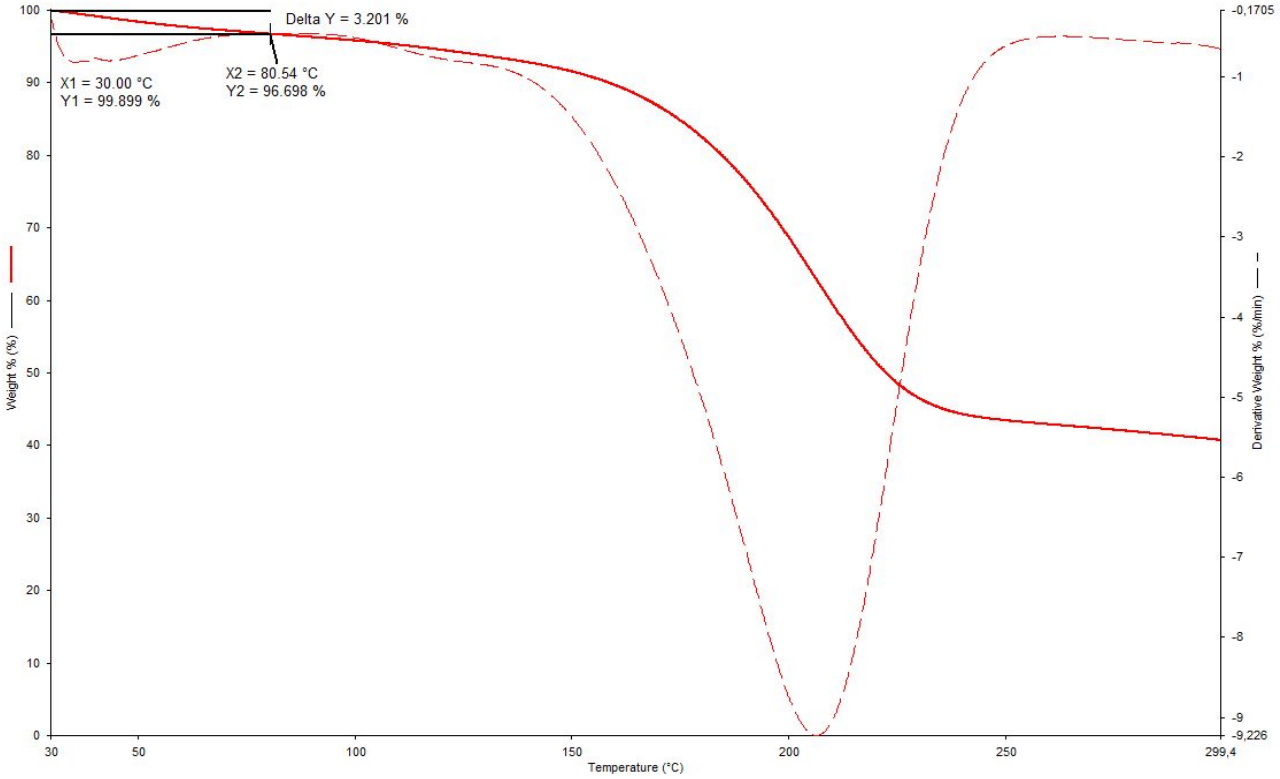

Figure S-7. TGA trace of **2**·2H_2O.

Variable-temperature powder XRD

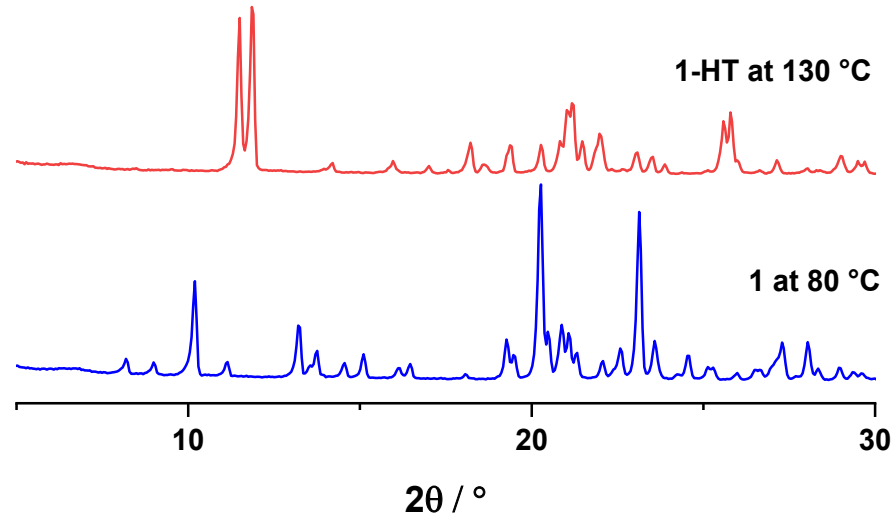

(a)

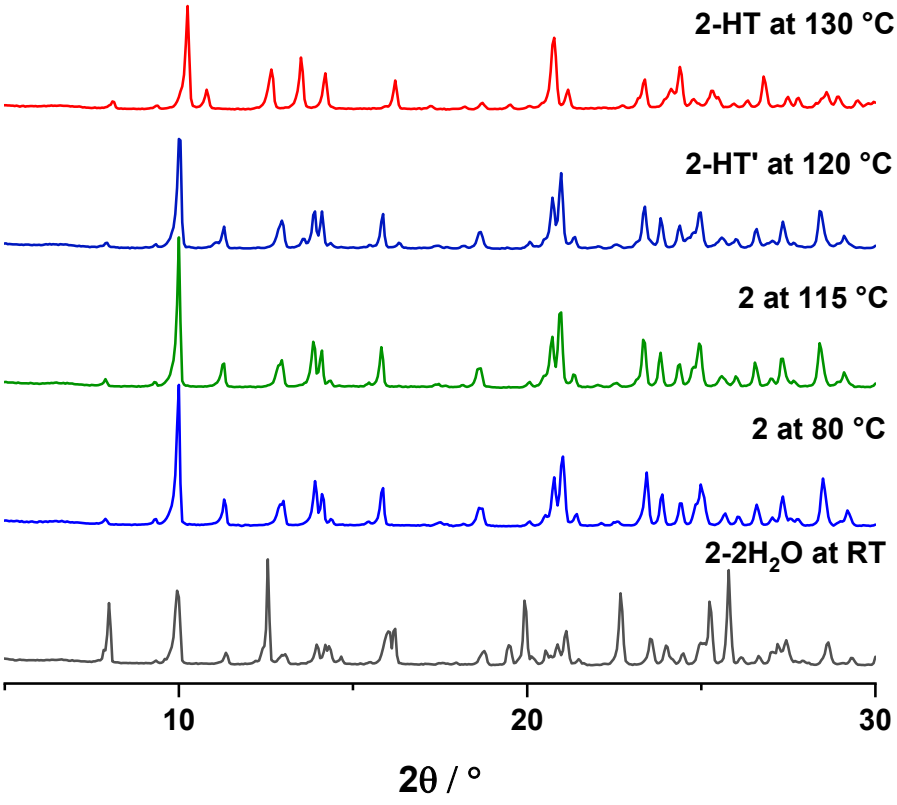

(b)

Figure S-8. Variable-temperature powder XRD experiments for: (a) compound **1** showing the patterns for the process **1** → **1-HT**, and (b) compound **2** showing the phase changes **2**·2H_2O → **2** → **2**-HT'→**2**-HT.

EIS details and Arrhenius plots

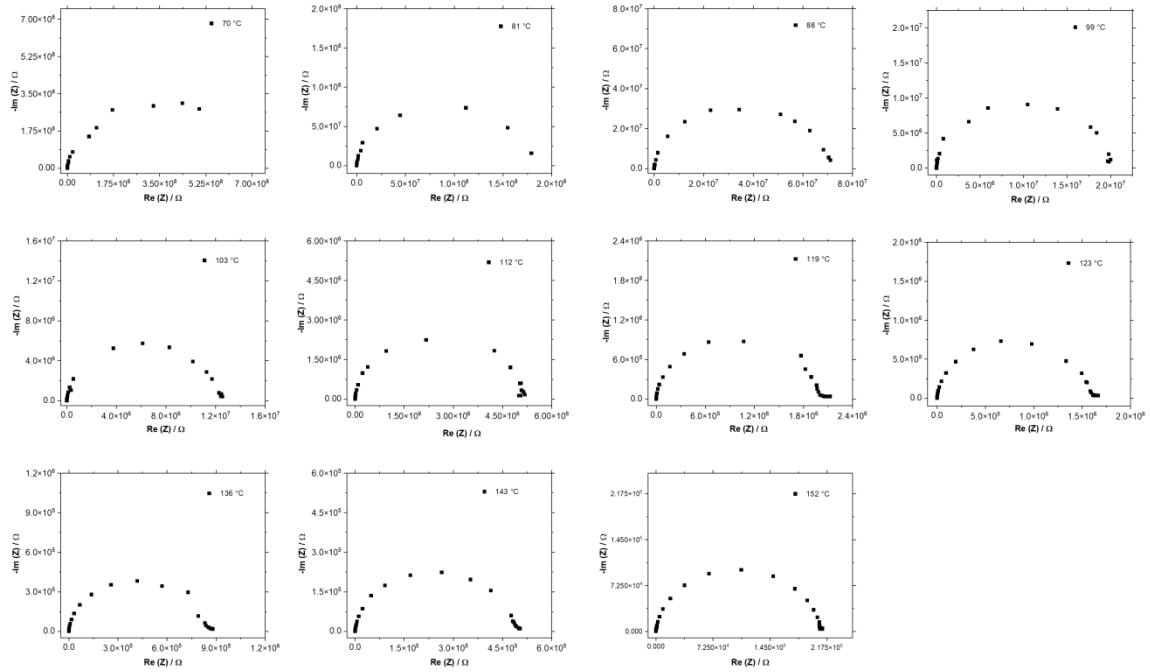

Figure S-9. Nyquist plots of 18-crown-6·$KHSO_4$ (**1**) at increasing temperature values.

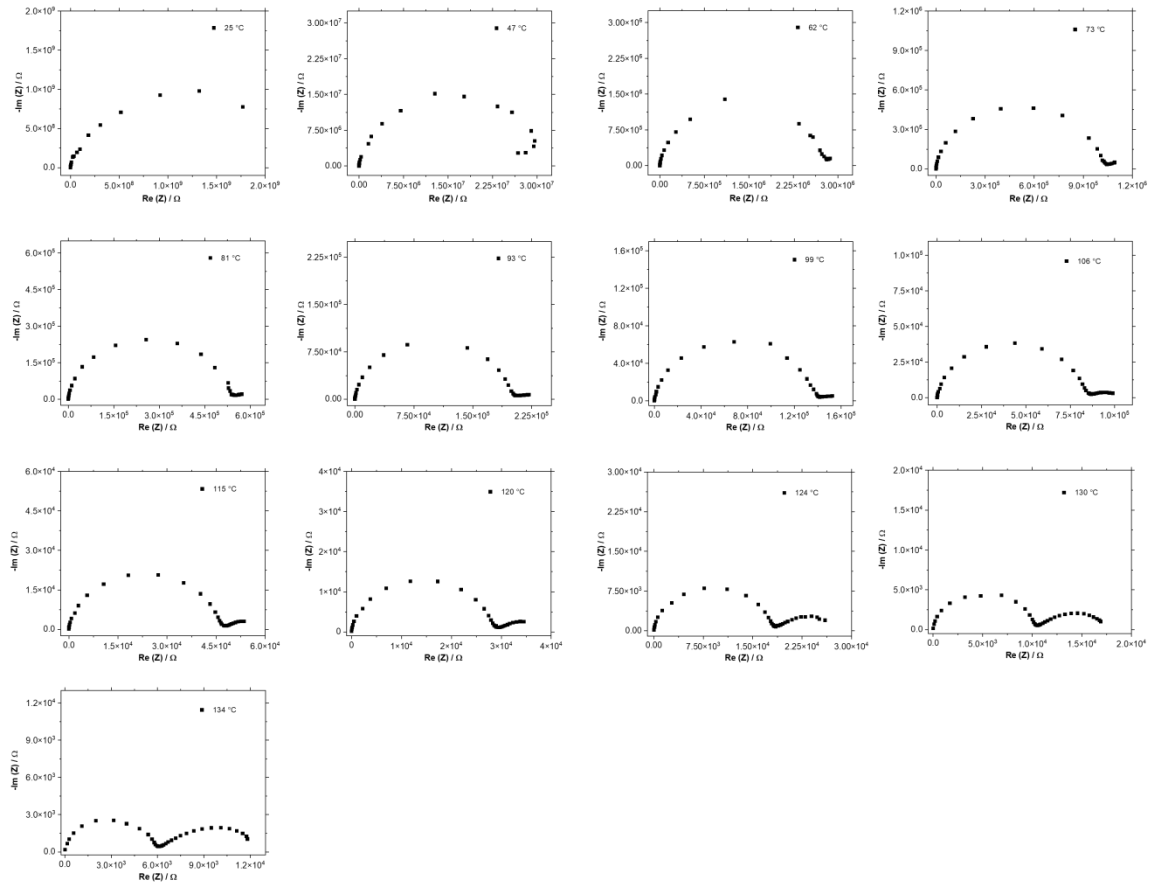

Figure S-10. Nyquist plots of 18-crown-6·$RbHSO_4$ (**2**) at increasing temperature values.

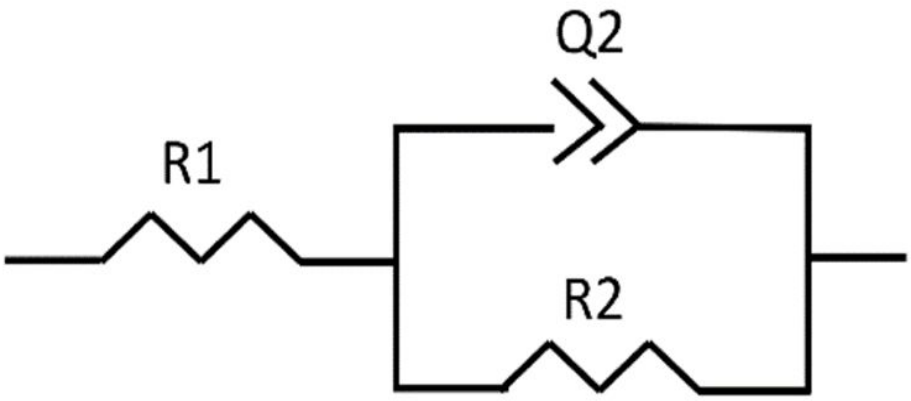

Figure S-11. Equivalent circuit used for fitting the electrochemical impedance spectra: R1 is related to the electronic resistance of the 2-electrode cell cables and blocking electrodes; R2 is the bulk ionic resistance of the pellet, and Q2 is the constant phase element that describes the double layer capacitance at the two ionic conductor/blocking electrode interfaces.

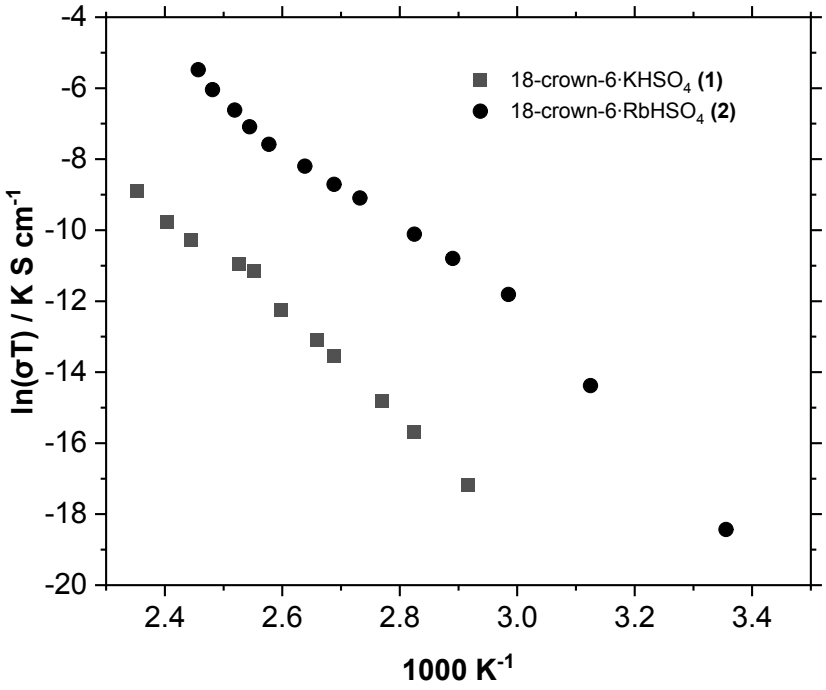

Figure S-12. Arrhenius plots of 18-crown-6·$KHSO_4$ (**1**), and 18-crown-6·$RbHSO_4$ (**2**).

Solid-state NMR

Table S-3. Operative temperatures (in °C) for the ^{1}H MAS and ^{1}H saturation recovery SSNMR experiments performed on **1** and **2** and corresponding ^{1}H T_1 values measured at the different temperatures.

Temperature (°C)	Measured ^{1}H T_1 (s)
1	
58	31.6
82	23.4
106	15.7
122	12.9
130	11.6
138	10.5
146	9.3
154	8.4
162	2.4
170	0.9
2	
58	33.8
82	20.5
106	20.0
122	16.8
126	16.1
130	15.3
134	14.5
138	13.4
146	11.2
154	9.2
162	7.0

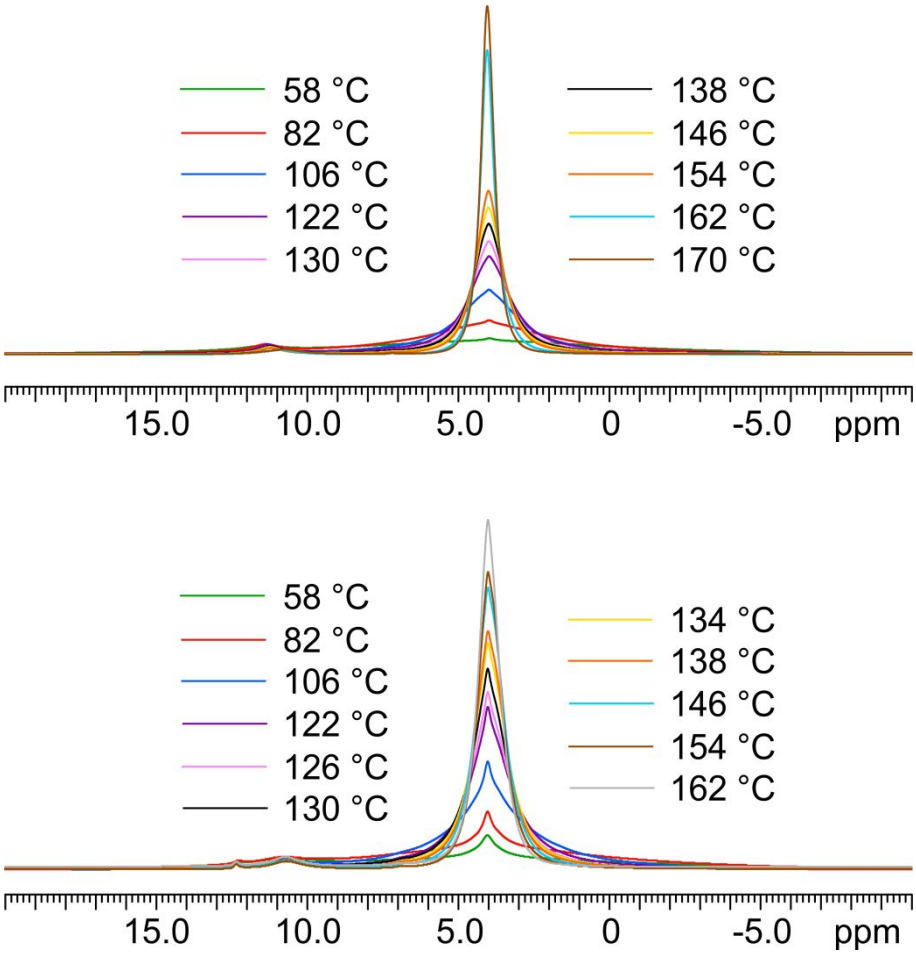

Figure S-13. ^{1}H (600.13 MHz) MAS SSNMR spectra of **1** (top) and **2** (bottom), acquired at the indicated temperatures at a spinning speed of 18 kHz.

References

(1) Braga, D.; Gandolfi, M.; Lusi, M.; Paolucci, D.; Polito, M.; Rubini, K.; Grepioni, F. Solution and Solid-State Preparation of 18-Crown[6] Complexes with M[HSO4]n Salts (M = NH4+, K +, Sr2+ and n = 1, 2) and an Investigation of Solvation/Desolvation Processes and Crystal Polymorphism. *Chem. Eur. J.* **2007**, *13* (18), 5249–5255.

(2) Itoh, K.; Moriyoshi, C. Structural Study of Phase Transition in Ferroelectric RbHSO4. *Ferroelectrics*; **2003**; Vol. 285, pp 91–104.